



University of Anbar



## Experimental and simulation investigation of porous Functionally Graded beam under bending loading

Muthanna Ismaeel Fayyadh<sup>a</sup>, Arz Y. Qwam Alden<sup>b</sup>

<sup>a,b</sup> Department of Mechanical Engineering , College of Engineering, University of Anbar, Al-Anbar, Iraq

### PAPER INFO

#### Paper history

Received: 03/04/2022

Revised: 04/05/2023

Accepted: 11/05/2023

#### Keywords:

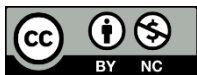
Beanding

Numerical Simulations

Porosity

Functionally Graded Materials

Difflection



Copyright: ©2023 by the authors. Submitted for possible open access publication under the terms and conditions of the Creative Commons Attribution (CC BY-NC 4.0) license.

<https://creativecommons.org/licenses/by-nc/4.0/>

### ABSTRACT

Due to their low weight and superior energy absorption, functionally graded porous structures have been used recently. In the fields of engineering, biomedicine, and aerospace, they have a variety of uses. Therefore, the researchers aim to reduce costs by balancing material strength and lightweight. To study the impact of the porosity gradient through thickness, samples of PLA material were designed and created using a 3D printer by international standard specifications. An experimental three-point bending test was performed, and then simulations were performed using ANSYS 2022 R1 software on samples with functionally gradient different porosity layers to verify the experimental results. The results from the experiment and the numerical values were aligned with an error rate of no more than 13%. The maximum bending load and maximum deflection of the beam were specified experimentally and compared with the numerical solution. The maximum bending on the minimum deflection When the porosity layer in the middle of the beam matched the ideal maximum bending load (190,194) N experimentally and numerically, respectively. The minimum deflection (5.9,6.4) mm experimentally and numerically, respectively, was obtained in samples with varying porous layers.

## 1. Introduction

In science and technology, the ability to exploit knowledge of material improvement is becoming an increasingly important factor in improving economic performance and social interest [1]. Modern porous materials engineering has dramatically changed design and construction. Porosity is common in materials, either due to the manufacturing process or intentional formation [2]. Functionally gradient porous materials (FGPM) are porous structures with a gradient porosity

distribution throughout their volume, as shown in Fig 1. Due to their remarkable weight strength and energy absorption option, these materials have acquired favor in numerous areas, including aerospace, marine, biomedical, automotive, and shipbuilding [3]. Due to their extraordinary characteristics, such as high bending toughness, lightweight, high sound absorption, and great damping performance, FGPMs have been widely used in mechanical and civil engineering throughout the past few decades[3]. Although the

\* Corresponding author: Muthanna Ismaeel Fayyadha; [mut20e2009@uoanbar.edu.iq](mailto:mut20e2009@uoanbar.edu.iq) ; +964-7819692103

presence of pores in FGPMs affects the rigidity of the entire structure, it also contributes to reducing the structure's weight. When evaluating the performance of FGPMs, it is crucial to consider their static and dynamic features [4].

Engineers and researchers have been challenged with the task of developing new materials to improve structural performance for many years. Despite these difficulties, due to their versatility in design strength and toughness, traditional laminated composite materials have become popular in various industries, including aircraft, aerospace, shipbuilding, and automobiles. However, these lamellar compounds can have performance limitations, particularly in thermoplastic applications, due to problems including dissociation, de-bonding, and residual stresses. The creation of FGM processes, which are advanced high-performance, multifunctional, and microscopically heterogeneous materials in the family of two- or more-stage engineering formulations, can help to overcome these limits. FGM is created by enabling a continuous, smooth change in the composition of matter in any direction utilizing various gradient rules (e.g., exponential laws, laws of force and sines). FGM is initially created to offer thermal resistance in fusion reactors and space structures [5]. Several researchers have developed functionally graded materials to solve the problems with laminated composites. Fig 1. depicts the advanced composite material hierarchy [6].

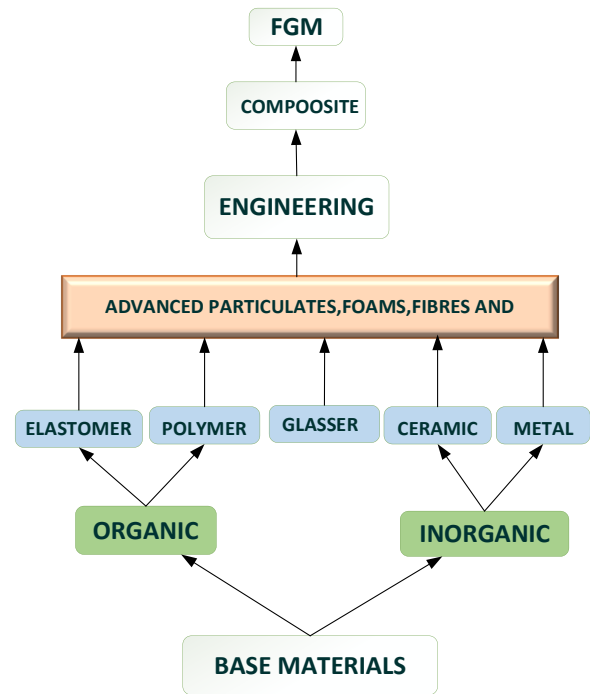


Figure 2. Hierarchy of advanced composite material [6]

The volume and weight fractions and their fluctuations can affect the orientation and geometry of these phases. Structures' volume fractions could be altered based on their thickness or in a different direction, such as along plates or shells. Mechanical parameters of FGM parts fluctuate in smooth, continuous, and desired directions, Young's modulus, thermal conductivity, Poisson's ratio, etc.

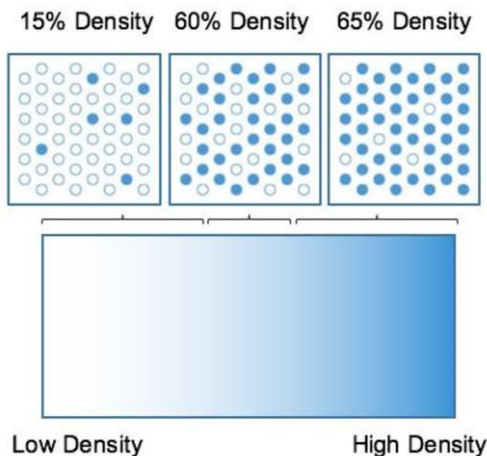


Figure 1. distribution of porosity through cross-sectional thickness of the sheet [14].

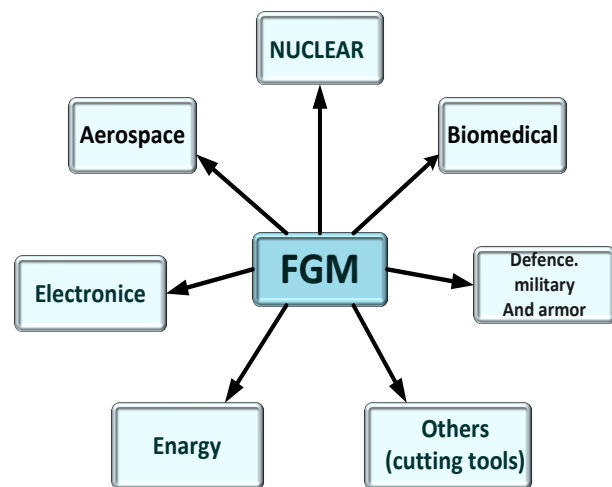


Figure 3. Uses of functionally graded materials(FGM) [7]

Due to its adaptability in personalizing material properties, FGM has grown and become somewhat attractive in recent years and is now considered an ideal material for a wide range of applications in industries including aerospace, nuclear engineering, and bioengineering [7]. Fig 3. illustrates a variety of FGM application areas. Nuclear, Biotechnology, and Space, while Fig 4. and Fig 5. respectively show some FGM parts suitable for automotive and aviation applications [8].

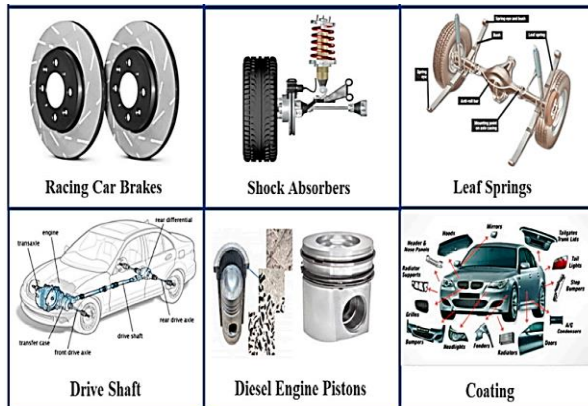


Figure 4. Automotive applications of FGMs parts [8].

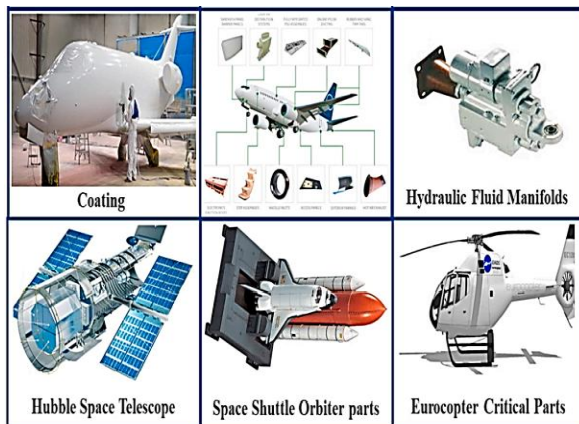


Figure 5. FGMs parts in aerospace applications [8].

## 2. Numerical Analysis

In this section, a functionally graded beam and plate with different porosity distributions are numerically modelled. Three-point beam bending was studied using ANSYS workbench (Version 2022 R1). The previous studies are validated using ANSYS. Furthermore, the results of the finite elements and experiments are validated. Experimental and numerical results indicate that there is a good agreement. Fig 6. shows the path that is used to write a paper

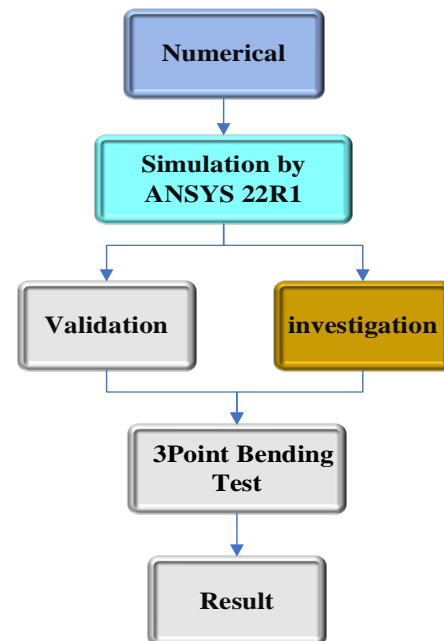


Figure 6. Flowchart for numerical solution.

## 3. Validation test

Three-point bending is a common test method used in materials science and engineering to determine the strength and stiffness of a material under bending forces. This test involves applying a load at two points on a material specimen while a third point acts as the support or fulcrum. The bending moment created by the load causes the material to deform, and the resulting deflection is measured as a function of the applied load. This test is widely used to specify the material properties required in various applications, such as in the aerospace, automotive, and construction industries. By accurately measuring the deflection and failure of materials under three-point bending, engineers and scientists can make informed decisions about the suitability of materials for specific applications and optimize the design and performance of structural components [9]. The results obtained by the researcher [3] is validated. The geometry of sandwich beam measuring 230 \*45 mm is applied as depicted in Figure 3.1. In the mesh, as shown in Figure 3.2 the number of nodes are (537107) and the number of elements are (112094). In addition, two metals were used, namely aluminium for the upper and lower parts and in the middle layer (core) PLA as shown in Table 1.

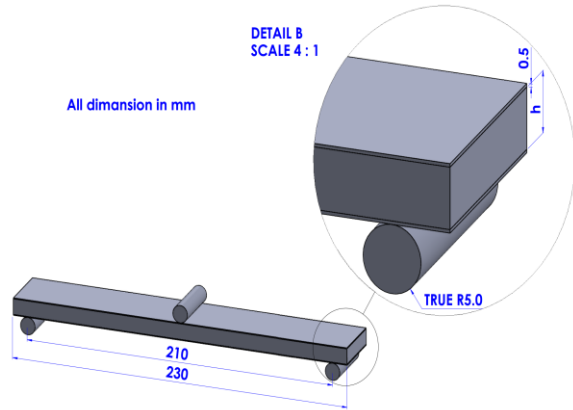


Figure 7. The geometry of validation

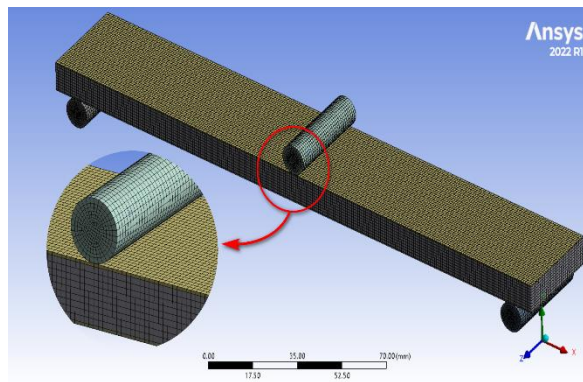


Figure 8. Mesh the geometry for validation

Table 1. Properties of the materials used by [3]

| Property                    | core (PLA) | Skin (AL- 6061-T6) |
|-----------------------------|------------|--------------------|
| E (GPa)                     | 1.2        | 70                 |
| $\rho$ (kg/m <sup>3</sup> ) | 1360       | 2702               |
| $\nu$                       | 0.38       | 0.30               |

The obtained results were verified with an error rate not exceeding 2.1 % for the deflection and 2% for the force. Fig 9. shows the contour for total deflection. And the Table 2 shows the section A is a results of the previous researcher [3] and section B is a results obtained from the analysis by the Ansys software.

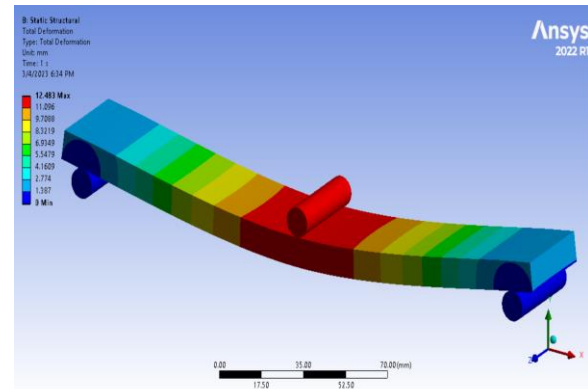


Figure 9. Counter for the total deflection

Table 2. Solution output for validation for beam

|             |                  | section A [3] |       |       |      | section B  |                             |             |                             |
|-------------|------------------|---------------|-------|-------|------|------------|-----------------------------|-------------|-----------------------------|
|             |                  | deflection    |       | Force |      | Present    | Error (Num and present) (%) |             | Error (Num and present) (%) |
| ( $\beta$ ) | FG core (h) (mm) | EXP.          | NUM.  | EXP.  | NUM. | deflection | Force                       | deformation | force                       |
| 0.1         | 10               | 13.8          | 12.45 | 573   | 670  | 12.48      | 680                         | 0.240384615 | 1.470588235                 |
| 0.1         | 20               | 9.56          | 8.72  | 2200  | 2445 | 8.83       | 2490                        | 1.245753114 | 1.807228916                 |
| 0.1         | 25               | 7.96          | 7.67  | 3830  | 4197 | 7.83       | 4252                        | 2.043422733 | 1.293508937                 |

## 4. Investigation Works

### 4.1 Experimental part

The samples for the bending test were prepared with dimensions according to the American specifications that prepared for the examination of materials (ASTM D790) [13]. Catalog (100x10x6 mm), and Fig 10. shows the standard dimensions for the bending test samples. The test was conducted with the same tensile device mentioned in Paragraph 4.2 , where the three points bending test was performed on the samples. From the device, obtain a load versus deflection curves. The results will be discussed in the next section. Fig 11 shows the bending samples before, during, and after the test.

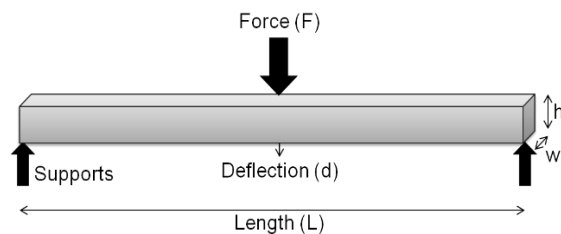


Figure 10. The standard dimensions of the bending sample [13].

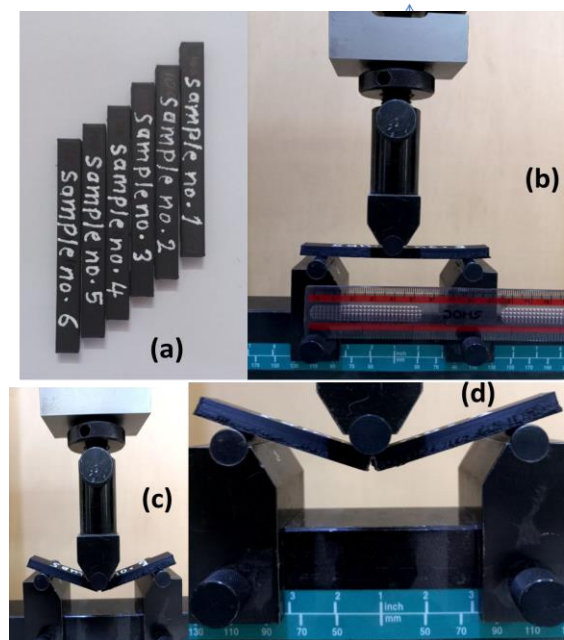


Figure 11. Preparing samples (a): before the test, (b) and (c) under the test, and (d) after failure

### 4.2 Numerical part

Three-point bending is a mechanical test used to determine the strength and elasticity of a material. It involves applying a force to a material sample at

two points while a third point is used to measure the deflection or deformation. The force is applied perpendicular to the sample, creating a bending moment that causes the material to bend. The force and deflection are measured to determine the material's bending strength and stiffness. This test is commonly used in the construction industry to evaluate the strength of structural materials like concrete, wood, and steel. It can also be used in other fields, like biomechanics, to study the properties of bones and other biological tissues [10].

In ANSYS analysis, there are three primary phases: designing the geometry, defining boundary conditions, obtaining results

#### 4.2.1 Geometry Design

At this stage, the design was divided into two phases. The first is to build a solid body (zero porous) by choosing the coordinate system, taking a sketch, and giving it dimensions, as shown in Fig 12. (a). The second phase divides the thickness by changing the porous layer, as shown in Fig 12. (b)

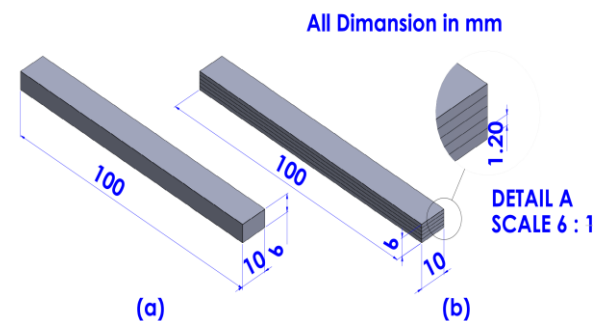


Figure 12. (a) solid body (zero porous), (b) layers with variable porous through the thickness

the materials shown in Table 3 were chosen and the Poisson ratio was taken 0.38 [7].

Table 3. The Material properties

| Porosity ( $\beta$ ) | E (GPa) | $\rho$ (kg/m <sup>3</sup> ) | $\nu$ |
|----------------------|---------|-----------------------------|-------|
| Zero                 | 1.64    | 1253.8                      | 0.38  |
| 0.1                  | 1.48    | 1128.42                     | 0.38  |
| 0.2                  | 1.312   | 1003.04                     | 0.38  |
| 0.3                  | 1.148   | 877.66                      | 0.38  |

#### 4.2.2 Geometry Mesh and the Boundary Conditions (B.C)

The concept underlying finite element analysis (FEA) involves dividing a problem into smaller, discrete elements that are solved individually and combined to obtain a comprehensive solution. The process of subdividing an object into smaller sections is known as meshing, and the solution's accuracy depends on the mesh's size. When modeling a beam in ANSYS, the mesh size for the elements must be chosen, and it directly impacts the speed and accuracy of the results. For the solid beam (zero porous), the FEM model consisted of 11530 elements and 67219 nodes, For the FGPM beam (0.1,0.2,0.3), the FEM model consisted of 6960 elements and 9304 nodes and boundary conditions was applied to the finite element analysis. The finite element model is presented in Fig 13.

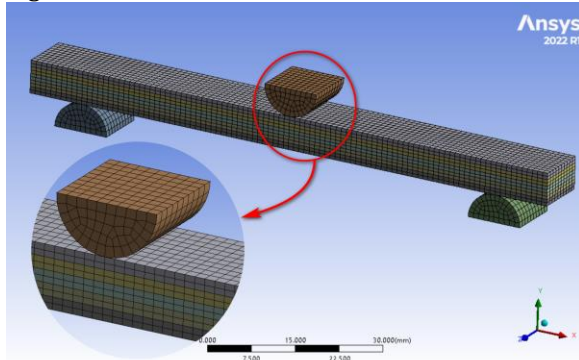


Figure 13. The Mesh generation in ANSYS of beam

### 5. Result

After conducting the test of the experimental part of the three-point bending of six samples containing layers with different porosities, the Fig (14–19) were obtained from the computer connected directly to the testing device, as shown in Fig 14. represents the solid sample, and Fig (15–19) represents the samples with different porous layers. From all the figures, the maximum bending load and the maximum bending Deflection were obtained for the samples.

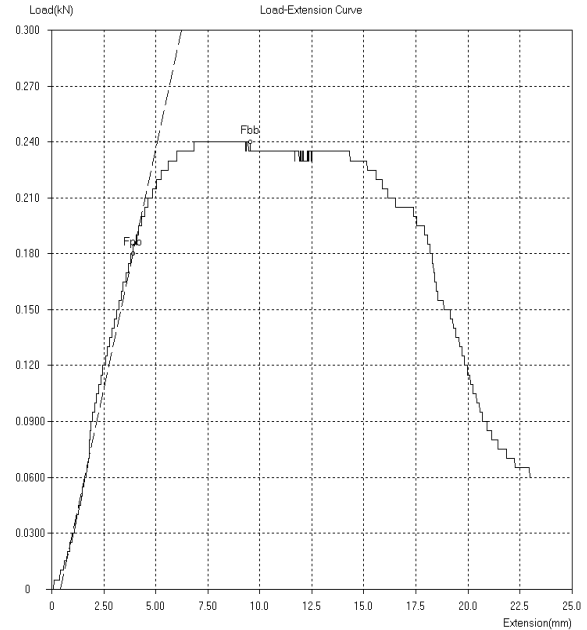


Figure 14. The Deflection with the force of the Non porous.

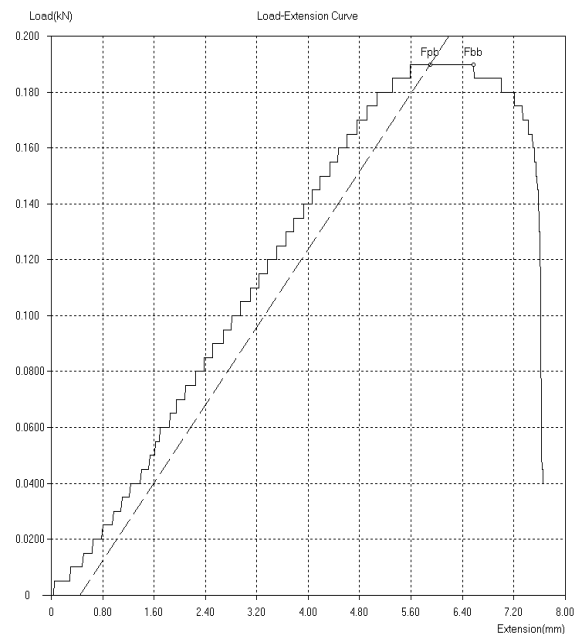


Figure 15. The Deflection with the force of the sample 1

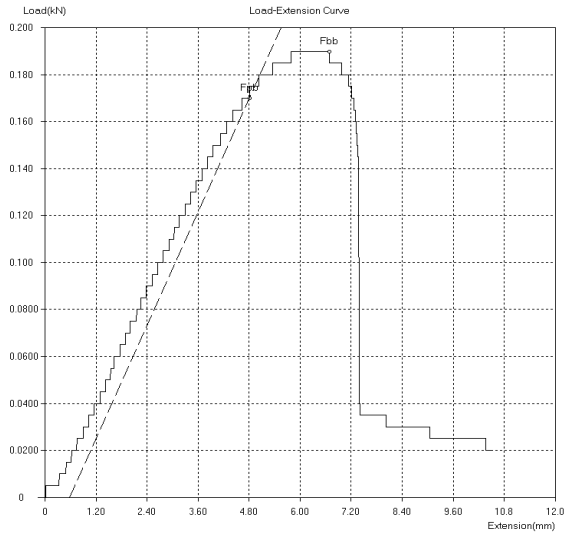


Figure 16. The Deflection with the force of the sample 2

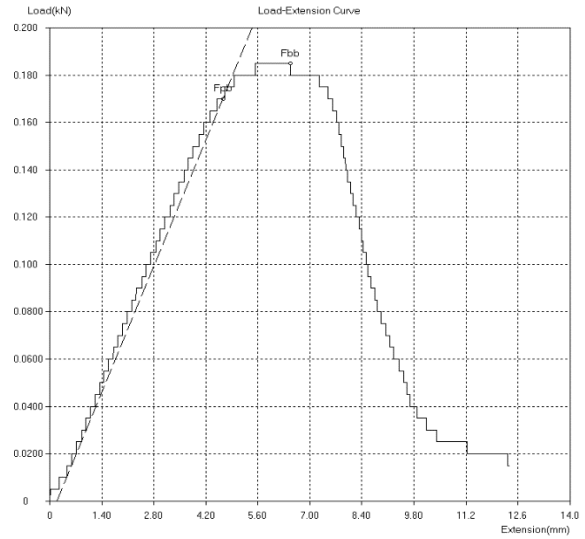


Figure 18. The Deflection with the force of the sample 4

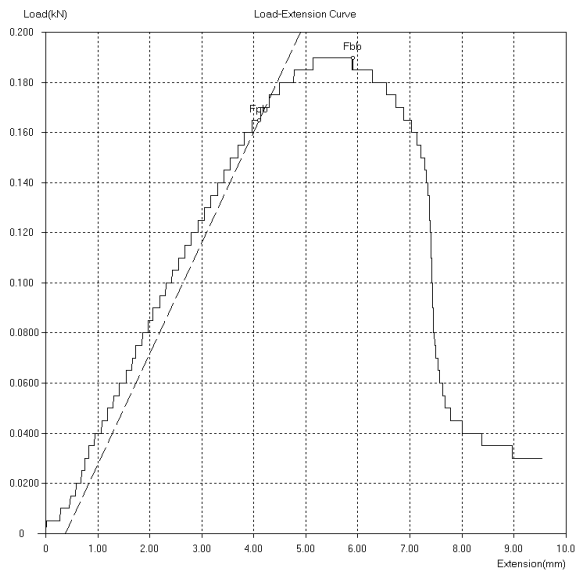


Figure .17 The Deflection with the force of the sample 3

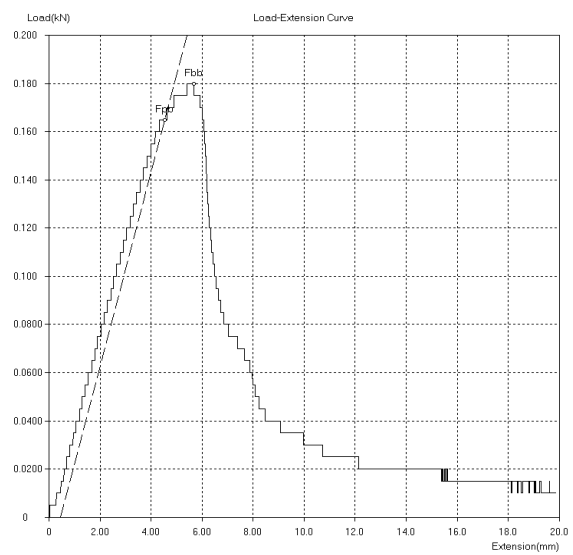


Figure 19. The Deflection with the force of sample 5

Fig 20. depicts a deflection counter for a solid sample and the experimental results were compared with the numerical results and the error percentage, as shown in Table 4. Fig (21-22) shows the maximum bending Deflection and the maximum bending load, respectively, for Non-porous samples and samples with variable porosity layers.

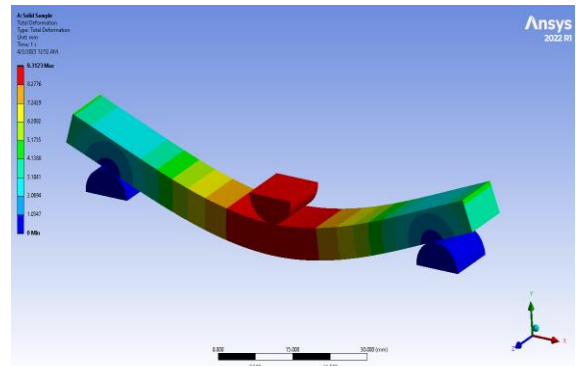
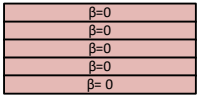
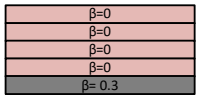
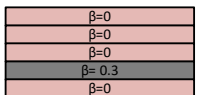
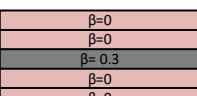
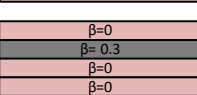
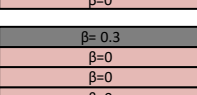
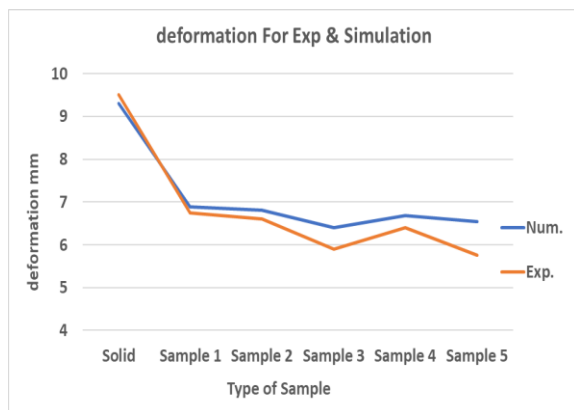


Figure 20. Counter for the total deflection for solid sample

**Table 4.** Comparing the numerical and experimental results and the percentage of error

| h (mm) | Case                | position of porous layer  | Porous ratio | Deflection (mm) |      | Force (N) |      | Deflection Error (Num and Exp.) (%) | Force Error (Num and Exp.) |
|--------|---------------------|---|--------------|-----------------|------|-----------|------|-------------------------------------|----------------------------|
|        |                     |   |              | Num.            | Exp. | Num.      | Exp. |                                     |                            |
| 10     | Zero porous (Solid) |    | 0            | 9.3             | 9.5  | 257       | 240  | 2.11                                | 6.61                       |
|        | Sample 1            |    |              | 6.88            | 6.75 | 191       | 190  | 1.93                                | 0.52                       |
|        | Sample 2            |    |              | 6.8             | 6.6  | 192       | 190  | 3.03                                | 1.04                       |
|        | Sample 3            |    | 0.3          | 6.4             | 5.9  | 194       | 190  | 8.47                                | 2.06                       |
|        | Sample 4            |    |              | 6.68            | 6.4  | 187       | 185  | 4.37                                | 1.07                       |
|        | Sample 5            |  |              | 6.54            | 5.75 | 181       | 180  | 13.74                               | 0.55                       |



**Figure 21.** Comparing the numerical and experimental results of the samples at the maximum bending deformation

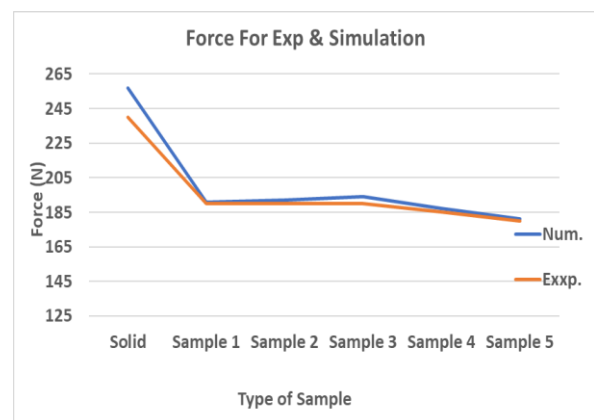


**Figure 22.** Comparing the numerical and experimental results of the samples at the maximum bending Force.

The load was applied at (180 N) for all samples to calculate the deflection value for each sample experimentally through the values and plots obtained from the experimental three-point bending test and numerically through the ANSYS



Software. The error ratio was calculated between the numerical and experimental tests, as shown in Table 5.

**Table 5.** Comparison of the results numerically and experimentally for diversion at constant load

| Case     | Porous ratio | Num. | Exp. | Error (%) |
|----------|--------------|------|------|-----------|
| Solid    | 0            | 3.64 | 3.85 | 5.45      |
| Sample 1 | 0.3          | 5.2  | 5.37 | 3.17      |
| Sample 2 |              | 5.1  | 5.24 | 2.67      |
| Sample 3 |              | 4.55 | 4.8  | 5.21      |
| Sample 4 |              | 5.12 | 5.3  | 3.40      |
| Sample 5 |              | 5.5  | 5.8  | 5.17      |

The results were compared to obtain the least deflection for the different porosity distributions of the samples at load 180 N, as shown in Fig 23.

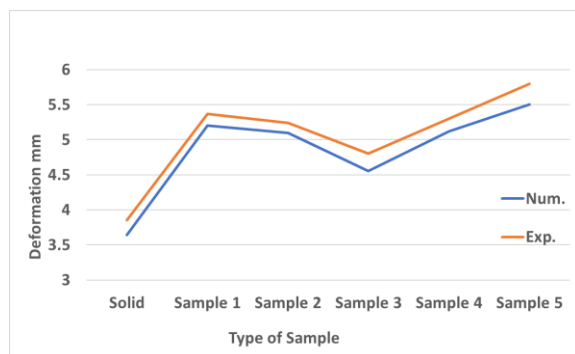


**Figure 23.** Comparing the numerical and experimental results of the samples at Force=180 N

## 6. Conclusion

This work presented the effect of porosity on the mechanical properties of structures such as beams. The desired target has been reached by changing the geometric coefficients, represented by changing the number of layers, porosity ratio, and layer thickness. This work was related to two parts: the experimental part and the numerical part. PLA material was used in this study.

Experimentally, various specimens were tested using three-point bending to specify the mechanical properties and comparison. Also, the mechanical properties were applied in the ANSYS

software to validate the experimental results. The following paragraphs summarize the most important obtained results:

Conclusion made by three-point bending tests the maximum load and deflection. The numerical solutions agreed well with the experimental tests, with an error rate not exceeding (13%). The maximum bending load and maximum bending deflection were found. When the porosity layer in the middle of the beam, corresponding to an optimum maximum bending load of (190,194)N experimental and numerical, respectively, and a maximum deflection of (5.9,6.4)mm experimental and numerical respectively. For samples with variable porosity layers.

The conclusion that was reached when a load of (180 N) was applied to all samples was to obtain the least deflection for the different porosity distributions of the samples, and its value was (4.55, 4.8) mm numerically and experimentally, respectively, when the porous layer was in the middle of the sample. The numerical solutions were found to agree with the experimental tests, with an error rate not exceeding (7%).

## Acknowledgements

We would like to express our deepest appreciation to [Dr.Arz, Dr.Mustafa, Dr.Emad] for their invaluable contributions to this research. This paper would not have been possible without their guidance, support, and encouragement. We also want to thank our families, friends, and colleagues for their understanding and patience throughout this project

## References

- [1] Awan U, Shamim S, Khan Z, Zia NU, Shariq SM, Khan MN. Big data analytics capability and decision-making: The role of data-driven insight on circular economy performance. *Technological Forecasting and Social Change* 2021;168:120766.
- [2] Gladysz GM, Chawla KK. Voids in materials: from unavoidable defects to designed cellular materials: Elsevier, 2020.
- [3] Njim EK, Bakhi SH, Al-Waily M. Experimental and numerical flexural properties of sandwich structure with functionally graded porous

- materials. Engineering and Technology Journal 2022;40(01):137-147.
- [4] Njim E, Bakhy S, Al-Waily M. Analytical and numerical free vibration analysis of porous functionally graded materials (FGPMs) sandwich plate using Rayleigh-Ritz method. Archives of Materials Science and Engineering 2021;110(1):27-41.
- [5] Vaka V, Sathujoda P, Yelike S. A review on dynamic analysis of porous functionally graded rotor systems. AIP Conference Proceedings: AIP Publishing LLC; 2021:020010.
- [6] Khan T, Zhang N, Akram A. State of the art review of functionally graded materials. 2019 2nd International Conference on Computing, Mathematics and Engineering Technologies (iCoMET): IEEE; 2019:1-9.
- [7] Mota A, Loja M. Mechanical behavior of porous functionally graded nanocomposite materials. C 2019;5(2):34.
- [8] Saleh B, Jiang J, Fathi R, et al. 30 Years of functionally graded materials: An overview of manufacturing methods, Applications and Future Challenges. Composites Part B: Engineering 2020;201:108376.
- [9] Lee K-J, Lee J-H, Jung C-Y, Choi E. Crack-closing performance of NiTi and NiTiNb fibers in cement mortar beams using shape memory effects. Composite Structures 2018;202:710-718.
- [10] Mandal T, Tinjum JM, Gokce A, Edil TB. Protocol for testing flexural strength, flexural modulus, and fatigue failure of cementitiously stabilized materials using third-point flexural beam tests: ASTM International, 2015.
- [11] Data AGM. Ansys Granta Materials Data | Unrivalled Materials Data Library. (<https://forum.ansys.com/forums/topic/what-is-the-source-of-mesh-quality-spectrum/>).
- [12] Forum AL. Ansys Innovation Space. (n.d.). 2022 (<https://forum.ansys.com/forums/topic/what-is-the-source-of-mesh-quality-spectrum/>).
- [13] ASTM S. Standard test methods for flexural properties of unreinforced and reinforced plastics and electrical insulating materials. ASTM D790. Annual book of ASTM standards 1997.
- [14] Loh, G.H., et al., An overview of functionally graded additive manufacturing. Additive Manufacturing, 2018. 23: p. 34-44.